Mat. Res. Soc. Symp. Proc. Vol. 661 © 2001 Materials Research Society

Silica Nano-particle Filled Poly(ethylene-ran-hexene)/xylene Gels

Howard Wang and Charles C. Han

National Institute of Standards and Technology, Polymers Division, Gaithersburg, MD 20899

The effect of silica nano-particle filler on poly(ethylene-co-hexene)/xylene gels has been investigated using mainly small angle neutron scattering and rheological measurements. Both non-filled and filled polymer gels show same characteristics in the structure factor and mechanical properties during melting and gelation. These observations suggest that particle interaction is screened by the absorbed polymers and the effect of the silica filler is mainly softening the gelation transition by introducing defects to the crosslinking microcrystals.

Introduction

Polymer gels are emerging as one of the most promising materials in the 21st century, having potential applications in many fields such as biomedical, pharmaceutical, chemical, and agricultural engineering. [1] Thermally reversible physical gels where crosslinking occurs either through specific interactions such as hydrogen bonding or microcrystals are considered particularly useful for biotechnology applications such as controlled drug release, [2] actuator, [3], artificial skin and organ. [4] Most studies on additives to gels focus on inclusion of the functionality [3, 5] or ion induced complexation [6], the effect of the nano-particle fillers on structure and properties of physical gels is not well understood. In this study we use mainly small angle neutron scattering (SANS) and dynamic mechanical analysis (DMA) to investigate the melting and gelation transitions in binary polymer/solvent, and ternary polymer/particle/solvent mixtures. The role of particle/solvent, polymer/solvent and particle/polymer interactions is discussed.

Materials and experiment

The gels in this study are either polymer in solvent or polymer and nano-particles in solvent. The polymer is a metallocene-catalyst synthesized statistic copolymer poly(ethylene-*ran*-hexene) (PEH), with a weight average molecular weight of 110 kg/mol and hexene comonomer content of 3 mol%, having a melting temperature of 127 ^{o}C. The primary silica nano-particles (SNP) are 10 nm in diameter. The specific surface area of

SNP is *ca.* 600 m^2/g. The particles were treated with $SiCl_2(CH_3)_2$ so that the surface is terminated with methyl groups. The hydrogenated xylene is a mixture of *o*-, *m*-, and *p*-type isomers, and has purity greater than 98% in volume, the perdeuteratered *o*-xylene (xyl) has purity greater than 99.3%.

Both non-filled and filled polymer gels were dispersed into homogeneous and transparent solutions in sealed vials at 130 ^oC. In both the SANS and DMA measurements, samples were loaded in sol state and allowed to form gels confined in the sample cells (2 mm thickness for SANS and 1 mm for DMA) upon cooling to room temperature. The SANS measurements were conducted when the samples are equilibrated at various temperatures during cycles of heating and cooling. The DMA were measured between parallel plates of 40 mm in diameter with a controlled stress of 10 Pa and frequency of 1 Hz, and at a temperature scan rate of 5 ^oC/min. The dilute solution of particles in solvent was sealed in a quartz banjo cell and measured by laser light transmission and small angle light scattering.

Results and discussion

The light transmission of the 2% mass fraction SNP in xylene (S2) at various temperatures is shown in Fig. 1(a). At temperatures lower than *ca*. 80 ^oC or higher than *ca*. 115 ^oC, the solution is flocculated and diminishes the light transmission, whereas at temperatures between 80 ^oC and 115 ^oC, the transmission is greater than 0.5 and the solution is transparent. The existence of the dissolution window is a consequence of

balancing the entropy of mixing and interactions of particle/particle and particle/solvent. At lower temperatures, the dissolution of the SNP aggregate upon temperature increase is due to increasing entropy of mixing. As temperature becomes higher and close to the boiling temperature of the solvent (*ca*. 140 ^{o}C), the particle-solvent interaction becomes less favorable due to the solvent density decrease, causing particles to aggregate. Figure 1(b) shows the fractal dimension D_f of the SNP aggregates at various temperatures at and around the dissolution window determined by small angle light scattering. D_f is analyzed through the relationship $S(q) \sim q^{D_f}$, where S(q) is the structure factor of the aggregates and q the amplitude of the momentum transfer vector. A constant value of *ca*. 1.5 is found in the entire temperature regime. The dimension of the SNP aggregates is temperature dependent while their fractal structure is insensitive to the temperature.

Figure 2(a) shows Lorentz-corrected SANS intensity Iq^2 as a function of the momentum transfer for 10 % mass fraction PEH gel (P10) at several temperatures during the first heating process. The scattering intensity decreases with temperature, and is quantified by calculating the SANS scattering invariant $Q_{\mathrm{SANS}} = \int I(q) * q^2 dq$ over the q range of the measurement 0.0078 A^{-1} to 0.075 A^{-1}. The invariant as a function of temperature during a heating-cooling-heating process is shown in Fig. 2(b). The arrows indicate the direction of the temperature variation. Figure 2(a) also shows a characteristic length increasing in its magnitude with temperature as indicated by scattering intensity peak shifting to the lower q. The characteristic length, $L = 2\pi / q_m$, where q_m is the peak value, is shown in the inset of Fig. 2(b). It is well known that the gels of semicrystalline polymer in solvent form upon crosslinking through fringed-micelle-like microcrystals,

and L reflects the long period of the lamella stacking. [8] As temperature increases, imperfect crystals melt, lamellae thin and the amorphous regions between the lamellae swell, resulting in increase of L and decrease of Q_{SANS}. The latter is related to the materials parameters through $Q_{SANS} \propto (d_a - d_c)^2 L_a L_c / L^2$, where the long period L is the sum of the amorphous layer thickness L_a and crystal thickness L_c, and d_a and d_c denote the scattering length density of the amorphous and crystal phase, respectively. At temperatures above 100 ^oC, the homogeneous sol is obtained, and Q_{SANS} vanishes. The opposite is observed when the mixture is cooled from the homogeneous sol. The hysteresis of both Q_{SANS} and L reflects the first order transition of crystallization/melting in the PEH/xyl mixture.

Similar measurement and analysis have been carried out on a gel with 10% mass fraction of polymer, 5% mass fraction of SNP in deuterated xylene (P10S5). Figure 3(a) shows the scattering curves at several temperatures during the first heating path. The Q_{SANS} and L are plotted in Fig. 3(b) and its inset, respectively. Compared to that of the non-filled gel, neutron scattering from filled gel shows the same characteristics, indicating essentially the identical origin of the gel formation, namely crosslinkage through the PEH microcrystals. Several differences upon SNP filling are observed: (1) a decrease of the scattering intensity, or Q_{SANS}, (2) a diminished hyteresis loop, (3) an increase in L and (4) a broadening in the transition region. These observations indicate that SNP additives introduce defects to both the crystals and the lamellar stacking as evidenced in the melting behavior and the scattering invariant. The increase in L suggests inclusion of the SNP in the inter-lamellar region. The lack of large-scale

particle mediated structures implies lack of the particle-particle interaction due to the polymer chain screening effect. Additional evidence of polymer chain adsorption to the particle surfaces came from the independent study on the neutron scattering contrast of binary and ternary mixtures. [9] Polymer adsorption has other important consequences: (1) the particles become neutral to polymers and are readily incorporated in polymer aggregates, (2) changes in the interfacial tension and the chain conformation at the particle surface causes shifting of the equilibrium melting temperature of the crystals around the particles, hence broadening of the gelation transition, and (3) micron-scale particle aggregates are prevented at higher temperatures resulting in homogeneous mixtures.

This picture is further supported by scan-temperature rheological measurements. Figure 4(a) and 4(b) plot dynamic storage modulus G', loss modulus G" and tangent of the phase angle, δ, for P10 and that with 2% mass fraction of SNP (P10S2), respectively. Both P10 and P10S2 gels display mechanical transition at about 95 ^{o}C, indicating breakdown of the network structure, consistent with the SANS measurement. G' spans 6 orders of magnitude between sol and gel states. It decreases exponentially below and above the transition, and drops abruptly at the transition, for about 2 orders of magnitude. The filled gel shows slight higher G' and G" at low temperatures indicating a certain degree of mechanical reinforcement, and a broader and more gradual mechanical property change around the transition. Approaching 80 ^{o}C, the non-filled gel shows slight upturn in G' and G", suggesting recrystallization occurring. On the contrary, filled gel display a drop of G' and G" below 80 ^{o}C, implying the beginning of the melting.

These observations are consistent with the model that the effect of the filler is mainly introducing defects and softening the transition.

The application considerations of the mechanical property change from step-wise to continuous response to temperature upon filler addition are as follows: the former can be used for devices requiring discrete output below and above a threshold, such as a switch; the latter can be used for continuous one-to-one responding devices.

Conclusions

The structure and properties of non-filled and filled PEH/xylene gels are investigated using small angle neutron scattering and dynamical mechanical analysis. Both gels contain microcrystals of the lamellar stacking as crosslinking points, and display crystallization and melting hysteresis. The silica nano-particle filler reduces the crystallinity, increases the long period of the lamellar stacking and suppresses the hysteresis loop. Rheological data also show filled-gel has a broader transition of mechanical properties than non-filled gels. We conclude that the particle-particle interaction is mostly screened out by the polymer chain adsorption to their surfaces and the effect of SNP filler is to introduce defects to polymer gel networks.

We acknowledge valuable discussions with Drs. Alan I. Nakatani, Erik K. Hobbie and Jack F. Douglas.

References

1). "Gels Handbook", Ed. Osada, Y. and Kajiwara, K., Academic Press. San Diego, (2000).

2). Lowe, T. L., Virtanen, J. and Tenhu, H., Polymer, 40, 2595 (1999).

3). Zrinyi, M., Colloid and Polymer Sci., 278, 98 (2000).

4). Suzuki, M. and Hirasa, O., Advances in Polymer Science, 110, 241 (1993).

5). Shibayama, M., Isaka, Y. and Shiwa, Y., Macromolecules, 32, 7086 (1999).

6). Shibayama, M., Takeuchi, T and Nomura S., Macromolecules, 27, 5350 (1994).

7). Certain equipment, instruments or materials are identified in this paper in order to adequately specify the experimental details. Such identification does not imply recommendation by the National Institute of Standards and Technology nor does it imply the materials are necessary the best for the purpose.

8.) "Introduction to Physical Polymer Science", Sperling, L. H., Jone Wikey & Sons Inc., New York, (1992).

9). Wang, H, unpublished.

Figure caption

Figure 1. (a) Light transmission on S2 at various temperatures shows a dissolution window between ca. 80 ^{o}C and 115 ^{o}C. (b) The fractal dimension D_f of the aggregates at and around the dissolution window shows a constant value of *ca*. 1.5.

Figure 2. (a) The Lorentz-corrected SANS intensity of P10 at various temperatures during the first heating process. The intensity decreases and peak position shifts to the

lower q as temperature increases. (b) Q_{SANS} as a function of temperature during heating and cooling cycles. The arrows indicate the direction of the temperature change. The inset shows the variation of the long period L, indicating swelling and condensing of the lamellar stacking upon heating and cooling, respectively.

Figure 3. (a) and (b) same as in Fig. 2 for P10S5.

Figure 4. The G', G'' and tanδ as a function of temperature for (a) P10 and (b) P10S2 showing sol-gel transition at around 95 ^{o}C. P10S2 shows a more gradual transition than P10.

Fig. 1 by Wang *et.*

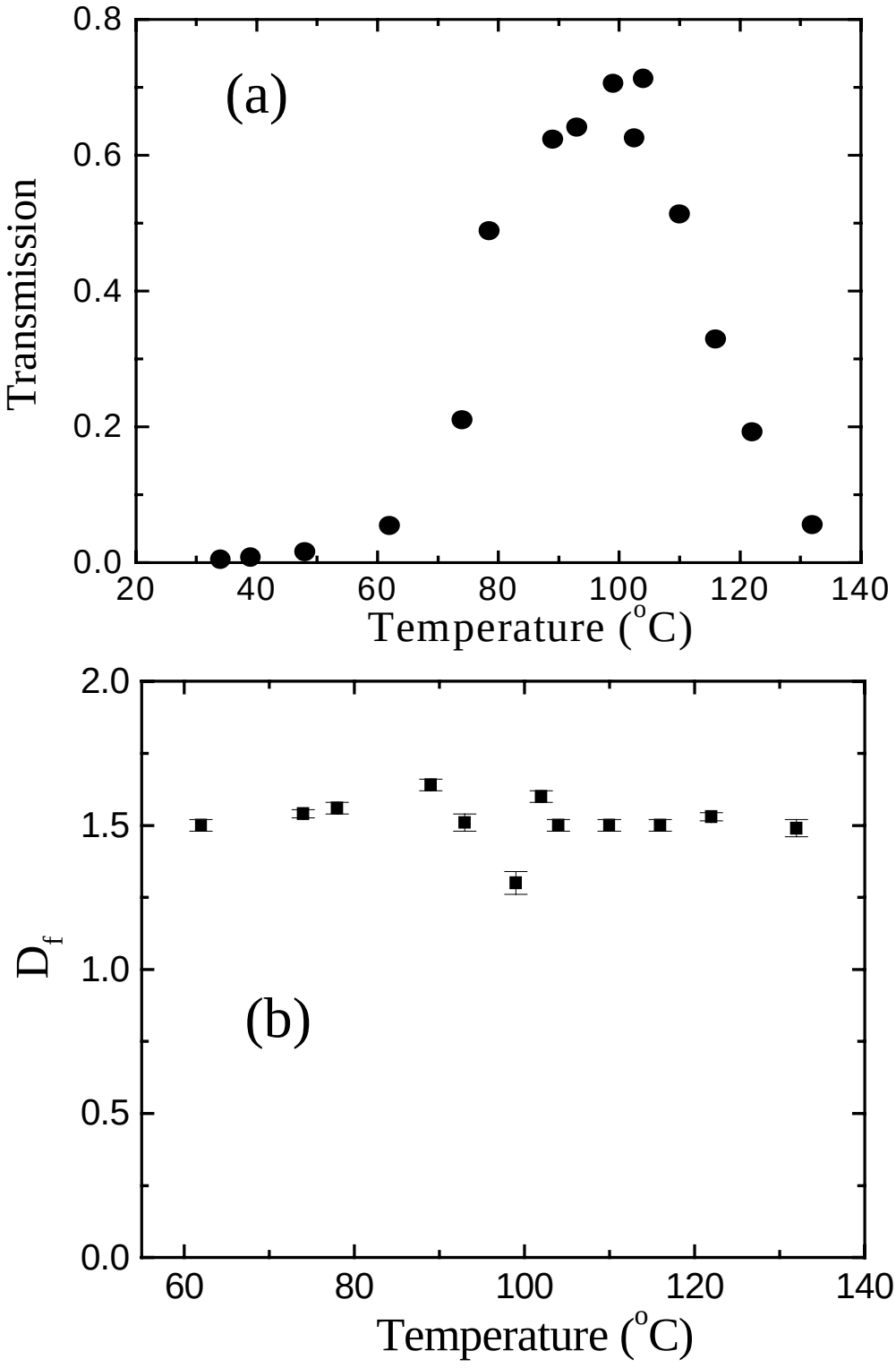

Fig. 2 by Wang *et. al.*

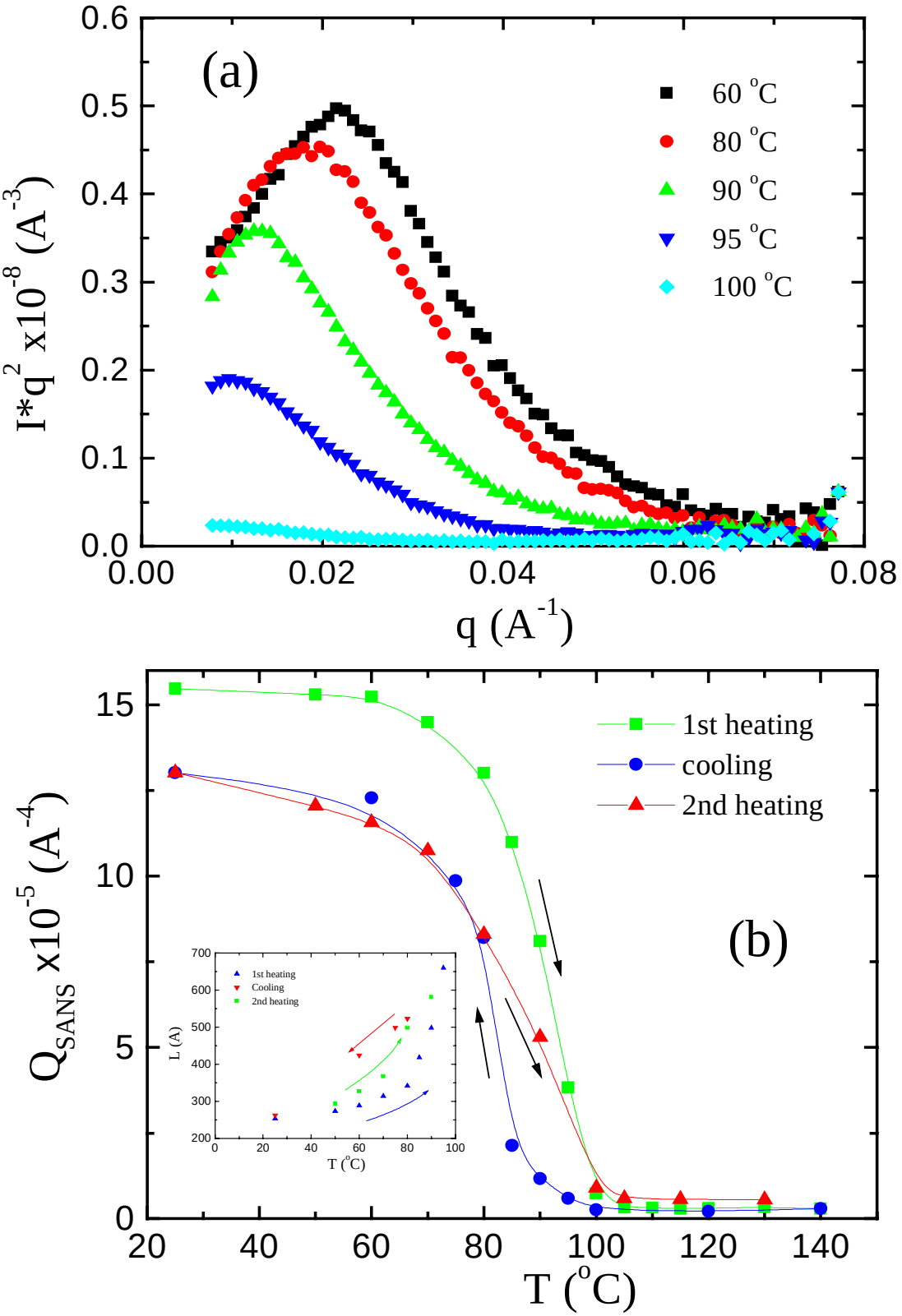

KK8.13.11

Fig. 3 by Wang *et.*

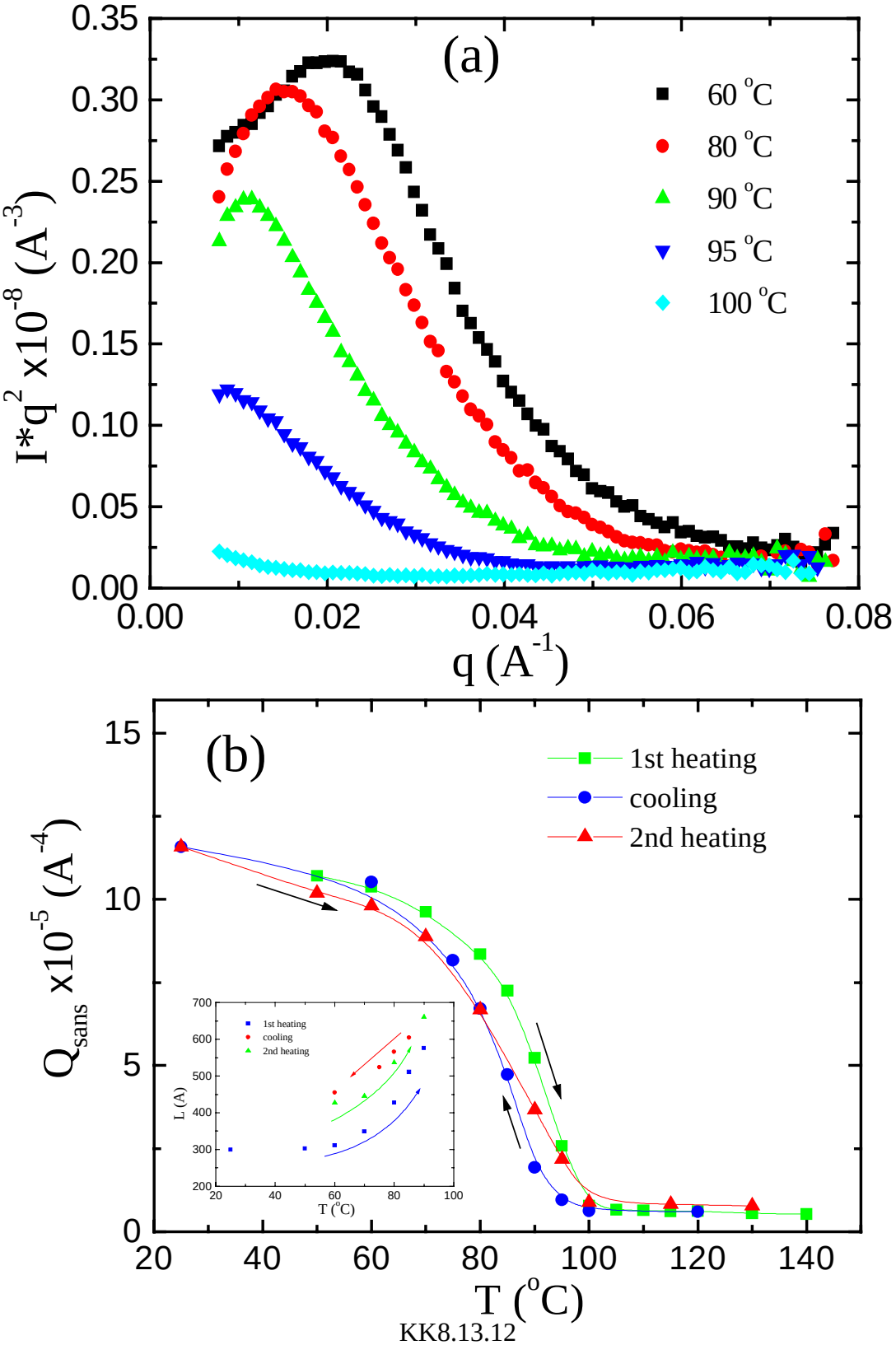

KK8.13.12

Fig. 4 by Wang *et. al.*

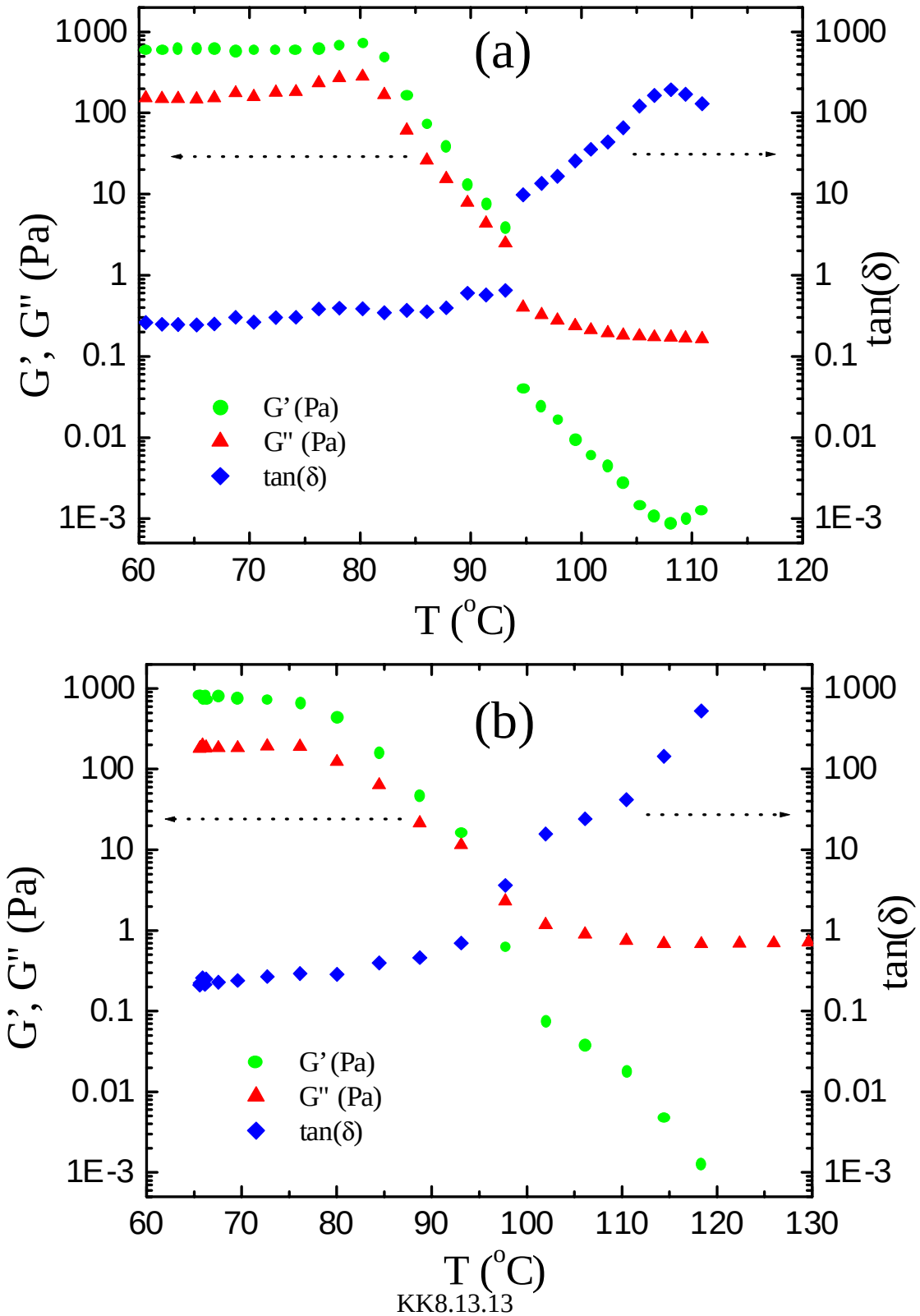

KK8.13.13